Solution to the Neumann problem exterior to a prolate spheroid by radial basis functions

Q.T. Le Gia [*] E. P. Stephan [†] T. Tran [*]

Dedicated to R.S. Anderssen on the occasion of his 70th birthday.

Abstract

We consider the exterior Neumann problem of the Laplacian with boundary condition on a prolate spheroid. We propose to use spherical radial basis functions in the solution of the boundary integral equation arising from the Dirichlet-to-Neumann map. Our approach is particularly suitable for handling of scattered data, e.g. satellite data. We also propose a preconditioning technique based on domain decomposition method to deal with ill-conditioned matrices arising from the approximation problem.

1 Introduction

In geophysical applications [4, 5], one is interested in the Neumann problem exterior to a spheroid where the orbits of satellites are located. The satellite creates data which amount to boundary conditions in scattered points. The consideration of spheroids provides a more realistic setting than spheres. It should be noted that satellite orbits are not located on one spheroid.

As a simple model problem, we consider here the Neumann problem for the Laplacian exterior to a prolate spheroid. A key tool of our approach is the use of the Dirichlet-to-Neumann map which directly converts the boundary value problem into a pseudodifferential equation on the spheroid. This integral equation is then handled with Fourier techniques by expansion into appropriate spherical harmonics. This approach was originally taken by Huang and Yu [6] who solved this pseudodifferential equation numerically with standard boundary elements on a regular grid on the angular domain of the spherical coordinates.

[*]School of Mathematics and Statistics, University of New South Wales, Sydney, NSW 2052, Australia. Email: qlegia@unsw.edu.au, Thanh.Tran@unsw.edu.au,

[†]Institut für Angewandte Mathematik and QUEST (Centre for Quantum Engineering and Space-Time Research), Leibniz Universität Hannover, Welfengarten 1, 30167 Hannover, Germany. Email: stephan@ifam.uni-hannover.de

Our approach uses spherical radial basis functions instead, allowing for better handling of scattered data. As the main result, we prove that if the solution is smooth then a high rate of convergence of the approximate solution can be achieved by choosing appropriate radial basis functions.

The paper is organised as follows. In Section 2, we report from [6] existence of the weak solution of the underlying boundary integral equation. In Section 3 we introduce the space of radial basis functions and prove an optimal a priori error estimate for the Galerkin approximation of the exact solution. In Section 4 we comment on the implementation with locally supported radial basis functions. The last section reports our numerical experiments which underly the theory.

2 Preliminary results

Let $\Gamma_0 = \{(x_1, x_2, x_3) \in \mathbb{R}^3 : \dfrac{x_1^2 + x_2^2}{b^2} + \dfrac{x_3^2}{a^2} = 1,\ a > b > 0\}$ be a prolate spheroid and Ω^c be the unbounded domain outside the boundary Γ_0. It is convenient to represent Γ_0 in prolate spheroidal coordinates (μ, θ, φ), which define a point $\boldsymbol{x} = (x_1, x_2, x_3) \in \mathbb{R}^3$ as

$$\begin{cases} x_1 &= f \sinh\mu \sin\theta \cos\varphi, \\ x_2 &= f \sinh\mu \sin\theta \sin\varphi, \\ x_3 &= f \cosh\mu \cos\theta, \end{cases}$$

where $f > 0$, $\mu \geq 0$, $\theta \in [0, \pi]$ and $\varphi \in [0, 2\pi)$. We note that this definition of prolate spheroidal coordinates is equivalent to that given in [1, p. 752] under the transformations $(\mu, \theta, \varphi) \mapsto (\xi, \eta, \phi)$ and $(x_1, x_2, x_3) \mapsto (x, y, z)$ where

$$\xi = \cosh\mu, \quad \eta = \cos\theta, \quad \phi = \varphi \quad \text{and} \quad x = x_3, \quad y = x_1, \quad z = x_2.$$

In prolate spheroidal coordinates (μ, θ, φ), a point $\boldsymbol{x} = (x_1, x_2, x_3) \in \Gamma_0$ can be represented as

$$\begin{cases} x_1 &= f_0 \sinh\mu_0 \sin\theta \cos\varphi, \\ x_2 &= f_0 \sinh\mu_0 \sin\theta \sin\varphi, \\ x_3 &= f_0 \cosh\mu_0 \cos\theta, \end{cases} \tag{2.1}$$

where $f_0 = \sqrt{a^2 - b^2}$, $a = f_0 \cosh\mu_0$, $b = f_0 \sinh\mu_0$, $\theta \in [0, \pi]$ and $\varphi \in [0, 2\pi)$.

We consider the exterior Neumann problem: given $g \in \Gamma_0$, find $U \in \Omega^c$ satisfying

$$\begin{cases} \Delta U &= 0 \quad \text{in } \Omega^c, \\ \partial_\nu U &= g \quad \text{on } \Gamma_0, \\ U(\boldsymbol{x}) &= O(\|\boldsymbol{x}\|^{-1}) \quad \text{as } \|\boldsymbol{x}\| \to \infty, \end{cases} \tag{2.2}$$

where $\|\boldsymbol{x}\|$ denotes the Euclidean norm of $\boldsymbol{x}$. Here ν denotes the unit outward normal vector on Γ_0.

Let $\Psi(\mu,\theta,\varphi) = F(\mu)G(\theta)H(\varphi)$ be such that $\Delta\Psi = 0$. Then, by using the method of separation of variables we have

$$\frac{d^2}{d\varphi^2}H(\varphi) + m^2 H(\varphi) = 0$$

$$\frac{1}{\sin\theta}\frac{d}{d\theta}(\sin\theta\frac{dG(\theta)}{d\theta}) - \frac{m^2 G(\theta)}{\sin^2\theta} + n(n+1)G(\theta) = 0,$$

$$\frac{1}{\sinh\mu}\frac{d}{d\mu}(\sinh\mu\frac{dF(\mu)}{d\mu}) - \frac{m^2 F(\mu)}{\sinh^2\mu} - n(n+1)F(\mu) = 0,$$

where m, n are integers. A solution for the above system is

$$\Psi_n^m(\mu,\theta,\varphi) = Q_n^m(\cosh\mu)Y_{nm}(\theta,\varphi), \quad m = -n,\dots,n; \quad n = 0,1,2,\dots$$

where $Q_n^m(x)$ are associated Legendre functions of the second kind (see [1, Chapter 8]) and $Y_{nm}(\theta,\varphi)$ are spherical harmonics of degree n (see [9]). The set of spherical harmonics

$$\{Y_{nm} : m = -n,\dots,n;\ n = 0,1,2,\dots\}$$

forms an orthonormal basis for $L^2(\mathbb{S}^2)$, where $\mathbb{S}^2$ is the unit sphere in $\mathbb{R}^3$.

Suppose $u(\theta,\varphi) := U(\mu_0,\theta,\varphi)$ is expanded into an absolutely convergent series

$$u(\theta,\varphi) = \sum_{n=0}^{\infty}\sum_{m=-n}^{n}\widehat{u}_{nm}Y_{nm}(\theta,\varphi)$$

where

$$\widehat{u}_{nm} = \int_0^{\pi}\int_0^{2\pi} u(\theta,\varphi)Y_{nm}^*(\theta,\varphi)\sin\theta\, d\varphi\, d\theta, \tag{2.3}$$

with Y_{nm}^* being the complex conjugate of Y_{nm}. Then the solution of the Laplace equation in the unbounded domain Ω^c outside Γ_0 is

$$U(\mu,\theta,\varphi) = \sum_{n=0}^{\infty}\sum_{m=-n}^{n}\frac{Q_n^m(\cosh\mu)}{Q_n^m(\cosh\mu_0)}\widehat{u}_{nm}Y_{nm}(\theta,\varphi), \quad \mu \geq \mu_0 > 0.$$

We note that

$$\left\|\frac{\partial \boldsymbol{x}}{\partial\mu}(\mu,\theta,\varphi)\right\| = f_0\sqrt{\cosh^2\mu - \cos^2\theta},$$

and hence the outward normal derivative $\partial_\nu U$ on Γ_0 can be computed as

$$\partial_\nu U(\theta,\varphi) = -\frac{1}{f_0\sqrt{\cosh^2\mu_0 - \cos^2\theta}}\frac{\partial U}{\partial\mu}(\mu_0,\theta,\varphi).$$

Therefore

$$\partial_\nu U(\theta,\varphi) = -\frac{1}{f_0\sqrt{\cosh^2\mu_0 - \cos^2\theta}}\sum_{n=0}^{\infty}\sum_{m=-n}^{n}\frac{\frac{dQ_n^m}{d\mu}(\cosh\mu_0)}{Q_n^m(\cosh\mu_0)}\widehat{u}_{nm}Y_{nm}(\theta,\varphi).$$

Let $\mathcal{K}$ denote the Dirichlet-to-Neumann map (or Steklov-Poincaré operator) defined for any $v \in H^{1/2}(\mathbb{S}^2)$ by

$$(\mathcal{K}v)(\theta,\varphi) := -\frac{1}{f_0\sqrt{\cosh^2\mu_0 - \cos^2\theta}} \sum_{n=0}^{\infty}\sum_{m=-n}^{n} \frac{\frac{dQ_n^m}{d\mu}(\cosh\mu_0)}{Q_n^m(\cosh\mu_0)} \widehat{v}_{nm} Y_{nm}(\theta,\varphi). \tag{2.4}$$

Then it is known that (see e.g. [12]) (2.2) is equivalent to

$$\mathcal{K}u = g \quad \text{ on } \Gamma_0. \tag{2.5}$$

Let $\mathcal{D}'(\Gamma_0)$ be the set of all distributions defined on Γ_0. The Sobolev spaces $H^s(\Gamma_0)$, $s \in \mathbb{R}$, are defined by

$$H^s(\Gamma_0) = \{f \in \mathcal{D}'(\Gamma_0) : \|f\|^2_{H^s(\Gamma_0)} = \sum_{n=0}^{\infty}\sum_{m=-n}^{n} (1+n^2)^s |\widehat{f}_{nm}|^2 < \infty\}.$$

The weak formulation for equation (2.5) is: Find $u \in H^{1/2}(\Gamma_0)$ satisfying

$$D(u,v) = \int_{\Gamma_0} gv \, \mathrm{d}s \quad \forall v \in H^{1/2}(\Gamma_0) \tag{2.6}$$

where

$$D(u,v) := \int_{\Gamma_0} (\mathcal{K}u)v \, \mathrm{d}s.$$

Since the measure on Γ_0 is $ds = f_0^2 \sinh\mu_0 \sqrt{\cosh^2\mu_0 - \cos^2\theta} \sin\theta \, d\theta \, d\varphi$ and the measure on the unit sphere $\mathbb{S}^2$ is $d\sigma = \sin\theta \, d\theta \, d\varphi$ we deduce from the definition of $D(u,v)$

$$\begin{aligned} D(u,v) &= f_0^2 \sinh\mu_0 \int_0^{2\pi}\int_0^{\pi} v(\theta,\varphi)(\mathcal{K}u)(\theta,\varphi)\sqrt{\cosh^2\mu_0 - \cos^2\theta} \sin\theta \, d\theta \, d\varphi \\ &= f_0^2 \sinh\mu_0 \int_{\mathbb{S}^2} v(\theta,\varphi)(\mathcal{K}u)(\theta,\varphi)\sqrt{\cosh^2\mu_0 - \cos^2\theta} \, d\sigma. \end{aligned}$$

By using (2.4) we obtain

$$D(u,v) = -f_0 \sinh\mu_0 \sum_{n=0}^{\infty}\sum_{m=-n}^{n} \frac{dQ_n^m(\cosh\mu_0)/d\mu}{Q_n^m(\cosh\mu_0)} \widehat{u}_{nm}\widehat{v}^*_{nm}.$$

Defining

$$H_n^m(x) := -\frac{(x^2-1)dQ_n^m(x)/dx}{Q_n^m(x)} \tag{2.7}$$

so that

$$H_n^m(\cosh\mu) = -\frac{dQ_n^m(\cosh\mu)/d\mu}{Q_n^m(\cosh\mu)} \sinh\mu,$$

we can rewrite $D(u, v)$ as

$$D(u, v) = f_0 \sum_{n=0}^{\infty} \sum_{m=-n}^{n} H_n^m(\cosh \mu_0) \widehat{u}_{nm} \widehat{v}_{nm}^*. \tag{2.8}$$

The following result is proved in [6]:

Theorem 2.1. *The bilinear form $D(\cdot, \cdot)$ is continuous and coercive on $H^{1/2}(\Gamma_0)$, i.e.,*

$$|D(u, v)| \leq \sqrt{2} f_0 x_0 \|u\|_{H^{1/2}(\Gamma_0)} \|v\|_{H^{1/2}(\Gamma_0)} \quad \forall u, v \in H^{1/2}(\Gamma_0),$$

and

$$\alpha \|v\|_{H^{1/2}(\Gamma_0)}^2 \leq D(v, v) \quad \forall v \in H^{1/2}(\Gamma_0),$$

where $x_0 = \cosh \mu_0 > 1$, $\alpha = (x_0^2 - 1)/x_0$ and f_0 are given in (2.1).

So by using Lax-Milgram theorem, there exists a unique solution for the variational problem (2.6).

In the following, we will approximate u by spherical radial basis functions (SRBFs).

3 Galerkin approximation using SRBFs

The finite dimensional subspaces that we shall use in our approximation are defined by using positive definite kernels on $\mathbb{S}^2$ and spherical radial basis functions.

A continuous function $\Phi : \mathbb{S}^2 \times \mathbb{S}^2 \to \mathbb{R}$ is called a *positive definite kernel* on $\mathbb{S}^2$ if it satisfies

(i) $\Phi(\boldsymbol{y}, \boldsymbol{z}) = \Phi(\boldsymbol{z}, \boldsymbol{y})$ for all $\boldsymbol{y}, \boldsymbol{z} \in \mathbb{S}^2$.

(ii) For any set of distinct scattered points $\{\boldsymbol{y}_1, \ldots, \boldsymbol{y}_K\} \subset \mathbb{S}^2$, the matrix $[\Phi(\boldsymbol{y}_i, \boldsymbol{y}_j)]$ is positive semi-definite.

If the matrix A is positive definite then Φ is called a *strictly positive definite* kernel; see [14, 19].

We define the kernel Φ from a univariate function $\phi : [-1, 1] \to \mathbb{R}$ by

$$\Phi(\boldsymbol{y}, \boldsymbol{z}) = \phi(\boldsymbol{y} \cdot \boldsymbol{z}) \quad \forall \boldsymbol{y}, \boldsymbol{z} \in \mathbb{S}^2, \tag{3.1}$$

where ϕ has a series expansion in terms of Legendre polynomials P_n of degree n, as

$$\phi(t) = \frac{1}{4\pi} \sum_{n=0}^{\infty} (2n+1) \widehat{\phi}(n) P_n(t). \tag{3.2}$$

Here

$$\widehat{\phi}(n) = 2\pi \int_{-1}^{+1} \phi(t) P_n(t) dt. \tag{3.3}$$

Due to the addition formula for spherical harmonics [9],

$$\sum_{m=-n}^{n} Y_{nm}(\boldsymbol{y})Y_{nm}^{*}(\boldsymbol{z}) = \frac{2n+1}{4\pi}P_n(\boldsymbol{y}\cdot\boldsymbol{z}),$$

the kernel Φ can be represented as

$$\Phi(\boldsymbol{y},\boldsymbol{z}) = \sum_{n=0}^{\infty}\sum_{m=-n}^{n} \widehat{\phi}(n)Y_{nm}(\boldsymbol{y})Y_{nm}^{*}(\boldsymbol{z}). \tag{3.4}$$

Remark 3.1. *In [2], a complete characterisation of strictly positive definite kernels on spheres is established: the kernel Φ is strictly positive definite if and only if $\widehat{\phi}(n) \geq 0$ for all $n \geq 0$ and $\widehat{\phi}(n) > 0$ for infinitely many even values of n and infinitely many odd values of n; see also [14] and [19]. In the following we assume that $\widehat{\phi}(n) > 0$ for all $n \geq 0$.*

The *native space* associated with the kernel Φ, which is defined by

$$N_\phi = \{v \in \mathcal{D}'(\mathbb{S}^2) : \sum_{n=0}^{\infty}\sum_{m=-n}^{n} \frac{|\widehat{v}_{nm}|^2}{\widehat{\phi}(n)} < \infty\},$$

is a reproducing kernel Hilbert space. Recalling the definition of Sobolev spaces on the sphere $\mathbb{S}^2$,

$$H^\tau(\mathbb{S}^2) = \{v \in \mathcal{D}'(\mathbb{S}^2) : \sum_{n=0}^{\infty}\sum_{m=-n}^{n} |\widehat{v}_{nm}|^2(1+n^2)^\tau < \infty\},$$

we can easily show that the native space N_ϕ is isomorphic to the Sobolev space $H^\tau(\mathbb{S}^2)$ when

$$\widehat{\phi}(n) \simeq (1+n^2)^{-\tau}. \tag{3.5}$$

Since the approximate solution to (2.6) is sought in a finite dimensional subspace of $H^{1/2}(\Gamma_0)$, in order to make use of the SRBFs we introduce the following bijection $\omega : \Gamma_0 \to \mathbb{S}^2$,

$$\omega(\boldsymbol{x}) = (\sin\theta\cos\varphi, \sin\theta\sin\varphi, \cos\theta), \tag{3.6}$$

where $\boldsymbol{x}$ is an arbitrary point on Γ_0 with prolate spheroidal coordinates

$$\boldsymbol{x}(\theta,\varphi) = (f_0\sinh\mu_0\sin\theta\cos\varphi, f_0\sinh\mu_0\sin\theta\sin\varphi, f_0\cosh\mu_0\cos\theta) \in \Gamma_0.$$

Using this map, we define a kernel on Γ_0 as

$$\Psi(\boldsymbol{x},\boldsymbol{x}') = \Phi(\omega(\boldsymbol{x}),\omega(\boldsymbol{x}')), \qquad \boldsymbol{x},\boldsymbol{x}' \in \Gamma_0,$$

where Φ is the kernel defined on $\mathbb{S}^2$; see (3.1). The kernel Ψ can be expanded into a series of spherical harmonics as

$$\Psi(\boldsymbol{x}, \boldsymbol{x}') = \sum_{n=0}^{\infty} \sum_{m=-n}^{n} \widehat{\phi}(n) Y_{nm}(\omega(\boldsymbol{x})) Y_{nm}^*(\omega(\boldsymbol{x}')). \tag{3.7}$$

Given a set of scattered points $X = \{\boldsymbol{x}_1, \ldots, \boldsymbol{x}_M\} \subset \Gamma_0$, we define V^τ by

$$V^\tau := \operatorname{span}\{\Psi_j := \Psi(\boldsymbol{x}_j, \cdot) : \boldsymbol{x}_j \in X\}. \tag{3.8}$$

The solution of (2.6) is approximated by $u_X \in V^\tau$ satisfying

$$D(u_X, v) = \int_{\Gamma_0} gv ds \quad \forall v \in V^\tau. \tag{3.9}$$

To this end, we have to solve a linear system

$$A\mathbf{c} = \mathbf{g} \tag{3.10}$$

where A is a matrix with entries

$$A_{i,j} = D(\Psi_i, \Psi_j), \quad i, j = 1, \ldots, M,$$

and $\mathbf{g}$ is a vector with entries

$$g_j = \int_{\Gamma_0} g\Psi_j ds, \quad j = 1, \ldots, M.$$

Using (2.8) and (3.7) we can write

$$A_{i,j} = f_0 \sum_{n=0}^{\infty} \sum_{m=-n}^{n} [\widehat{\phi}(n)]^2 H_n^m(\cosh \mu_0) Y_{nm}(\omega(\boldsymbol{x}_i)) Y_{nm}^*(\omega(\boldsymbol{x}_j)). \tag{3.11}$$

The positive definiteness of the matrix A is a direct consequence of coercivity of the bilinear form $D(\cdot, \cdot)$ established in Theorem 2.1. In the calculation we use the truncated version of $D(u, v)$ defined by

$$D_N(u, v) = f_0 \sum_{n=0}^{N} \sum_{m=-n}^{n} H_n^m(\cosh \mu_0) \widehat{u}_{nm} \widehat{v}_{nm}^*, \tag{3.12}$$

so that the matrix A is approximated by $A^{(N)}$ with entries

$$A_{i,j}^{(N)} = f_0 \sum_{n=0}^{N} \sum_{m=-n}^{n} [\widehat{\phi}(n)]^2 H_n^m(\cosh \mu_0) Y_{nm}(\omega(\boldsymbol{x}_i)) Y_{nm}^*(\omega(\boldsymbol{x}_j)).$$

We have to choose a sufficient large N ($N = 100$ is used in our numerical experiments) to guarantee positive definiteness of the matrix $A^{(N)}$. This is termed a "variational crime" by Strang and Fix [15] and will be discussed later in the error analysis.

The integral

$$\int_{\Gamma_0} g\Psi_j \,\mathrm{d}s = f_0^2 \sinh\mu_0 \int_0^{\pi}\int_0^{2\pi} g(\theta,\phi)\sqrt{\cosh^2\mu_0 - \cos\theta}\;\Psi_j(\theta,\varphi)\sin\theta\, d\varphi\, d\theta$$

can be evaluated by an appropriate cubature on the sphere $\mathbb{S}^2$ (e.g. [3]), or by using the Fourier expansions of g and Ψ_j.

Let $Y = \{\boldsymbol{y}_1, \ldots, \boldsymbol{y}_M\}$ be the image of X under the map ω, i.e., $\boldsymbol{y}_j = \omega(\boldsymbol{x}_j)$ for $j = 1, \ldots, M$. As Y is a set of scattered points on $\mathbb{S}^2$, we define the mesh norm h_Y of Y as usual,

$$h_Y = \sup_{\boldsymbol{y}\in\mathbb{S}^2} \min_{\boldsymbol{y}_j\in Y} \cos^{-1}(\boldsymbol{y}\cdot\boldsymbol{y}_j).$$

We have the following approximation property:

Theorem 3.2. *Assume that* (3.5) *holds for* $\tau > 1$. *If* $f \in H^s(\Gamma_0)$ *for* $s \le 2\tau$, *then for* $t \le \min\{s,\tau\}$, *there exists* $\eta \in V^\tau$ *so that*

$$\|f - \eta\|_{H^t(\Gamma_0)} \le c h_Y^{s-t} \|f\|_{H^s(\Gamma_0)},$$

where c *is a positive constant independent of* Y.

Proof. For any function $f \in H^\tau(\Gamma_0)$, if $F(\boldsymbol{y}) = f(\omega^{-1}(\boldsymbol{y}))$ then F is a function in $H^\tau(\mathbb{S}^2)$ and

$$\widehat{F}_{nm} = \widehat{f}_{nm} = \int_0^{\pi}\int_0^{2\pi} f(\theta,\varphi)\sin\theta\, d\varphi\, d\theta.$$

Hence

$$\|f\|^2_{H^s(\Gamma_0)} = \sum_{n=0}^{\infty}\sum_{m=-n}^{n} (1+n^2)^s |\widehat{F}_{nm}|^2 = \|F\|^2_{H^s(\mathbb{S}^2)}. \tag{3.13}$$

Using the result in Theorem 3.7 [16] (see also Remark 5.1 therein), there exists $\tilde{\eta} \in$ span $\{\Phi(\boldsymbol{y}_j,\cdot) : j = 1, \ldots, M\}$ so that

$$\|F - \tilde{\eta}\|_{H^t(\mathbb{S}^2)} \le c h_Y^{s-t} \|F\|_{H^s(\mathbb{S}^2)}.$$

Defining $\eta(\boldsymbol{x}) := \tilde{\eta}(\omega(\boldsymbol{x}))$ and using (3.13) we deduce the required result, noting that $\eta \in V^\tau$. □

Theorem 3.3. *Assume that the exact solution* u *is in* $H^s(\Gamma_0)$ *for some* $s > 1/2$ *and the approximate solution* u_X *is constructed from* $V^\tau = span\{\Psi_j = \Psi(\boldsymbol{x}_j,\cdot) : j = 1, \ldots, M\}$ *where* Ψ *is defined from a kernel so that* (3.5) *holds for* $\tau > s+1$. *Then*

$$\|u - u_X\|_{H^{1/2}(\Gamma_0)} \le C(h_Y^{s-1/2} + N^{-2s+1}\sqrt{M})\|u\|_{H^s(\Gamma_0)},$$

where the constant C is independent from N and the set X used to define Ψ_j. In particular, if N is chosen to be proportional to M^γ with $\gamma > 1/(4s-2)$ then

$$\|u - u_X\|_{H^{1/2}(\Gamma_0)} \le C(h_Y^{s-1/2} + M^{\gamma(-2s+1)+1/2})\|u\|_{H^s(\Gamma_0)},$$

which assures the convergence of the approximation.

Proof. By using Strang Lemma [15], we have the following estimate

$$\|u - u_X\|_{H^{1/2}(\Gamma_0)} \le \inf_{v\in V^\tau} \|u - v\|_{H^{1/2}(\Gamma_0)} + \max_{v\in V^\tau} \frac{|D_N(u,v) - D(u,v)|}{[D_N(v,v)]^{1/2}}. \tag{3.14}$$

Theorem 3.2 gives an estimate for the first term on the right-hand side:

$$\inf_{v\in V^\tau} \|u - v\|_{H^{1/2}(\Gamma_0)} \le c h_Y^{s-1/2}\|u\|_{H^s(\Gamma_0)}.$$

To estimate the second term on the right-hand side, firstly we notice that (see [6])

$$\frac{(x^2-1)}{x}(1+n^2)^{1/2} < H_n^m(x) < \sqrt{2}(1+n^2)^{1/2}x \quad \text{and} \quad H_n^{-m}(x) = H_n^m(x) \tag{3.15}$$

for $x > 1$, $m = 0, \dots, n$, and $n = 0, 1, 2, \dots$. This estimate and the Cauchy-Schwarz inequality yield

$$\begin{aligned}
|D_N(u,v) - D(u,v)| &= \left| f_0 \sum_{n=N+1}^{\infty} \sum_{m=-n}^{n} H_n^m(\cosh\mu_0)\widehat{u}_{nm}\widehat{v}^*_{nm} \right| \\
&\le \alpha_1 \sum_{n=N+1}^{\infty} \sum_{m=-n}^{n} (1+n^2)^{1/2}|\widehat{u}_{nm}|\,|\widehat{v}^*_{nm}| \\
&\le \alpha_1 \left(\sum_{n=N+1}^{\infty} \sum_{m=-n}^{n} (1+n^2)^{1/2}|\widehat{u}_{nm}|^2 \right)^{1/2} \\
&\quad \left(\sum_{n=N+1}^{\infty} \sum_{m=-n}^{n} (1+n^2)^{1/2}|\widehat{v}_{nm}|^2 \right)^{1/2},
\end{aligned}$$

where $\alpha_1 = \sqrt{2} f_0 \cosh\mu_0$. It follows from

$$\sum_{n=N+1}^{\infty} \sum_{m=-n}^{n} (1+n^2)^{1/2}|\widehat{u}_{nm}|^2 \le (1+N^2)^{-s+1/2}\|u\|^2_{H^s(\Gamma_0)} \quad \forall u \in H^s(\Gamma_0),\ s > 1/2,$$

that

$$|D_N(u,v) - D(u,v)| \le \alpha_1(1+N^2)^{-s+1/2}\|u\|_{H^s(\Gamma_0)}\|v\|_{H^s(\Gamma_0)}.$$

On the other hand there holds

$$D_N(v,v) \ge D_0(v,v) \ge \alpha_2|\widehat{v}_{00}|^2,$$

wherer $\alpha_2 = (\cosh^2\mu_0 - 1)/\cosh\mu_0$. Therefore, we can bound the second term on the right-hand side of the inequality (3.14) as follows:

$$\max_{v\in V^\tau}\frac{|D_N(u,v)-D(u,v)|}{[D_N(v,v)]^{1/2}} \le \frac{\alpha_1}{\sqrt{\alpha_2}}(1+N^2)^{-s+1/2}\|u\|_{H^s(\Gamma_0)}\max_{v\in V^\tau}\frac{\|v\|_{H^s(\Gamma_0)}}{|\widehat{v}_{00}|}. \tag{3.16}$$

Since $v \in V^\tau$, we write v as $v = \sum_{j=1}^{M}\beta_j\Psi_j$ and have

$$\|v\|^2_{H^s(\Gamma_0)} = \sum_{i=1}^{M}\sum_{j=1}^{M}\beta_i\beta_j(\Psi_i,\Psi_j)_{H^s(\Gamma_0)} \quad\text{and}\quad |\widehat{v}_{00}|^2 = \frac{|\widehat{\phi}(0)|^2}{4\pi}\left(\sum_{j=1}^{M}\beta_j\right)^2.$$

Thus, letting $\beta = (\beta_1,\ldots,\beta_M)^T$ and letting B be the matrix with entries $B_{i,j} = (\Psi_i,\Psi_j)_{H^s(\Gamma_0)}$, we obtain

$$\max_{v\in V^\tau}\frac{\|v\|^2_{H^s(\Gamma_0)}}{|\widehat{v}_{00}|^2} = \frac{4\pi}{|\widehat{\phi}(0)|^2}\max_{\beta\in\mathbb{R}^M}\frac{\beta^TB\beta}{\beta^T\beta} = \frac{4\pi}{|\widehat{\phi}(0)|^2}\lambda_{\max}(B), \tag{3.17}$$

where $\lambda_{\max}(B)$ denotes the maximum eigenvalue of the matrix B. We can view B as an interpolation matrix generated by the following strictly positive definite kernel (see Remark 3.1)

$$\Pi(\boldsymbol{x},\boldsymbol{y}) = \sum_{n=0}^{\infty}\sum_{m=-n}^{n}[\widehat{\phi}(n)]^2(1+n^2)^sY_{nm}(\omega(\boldsymbol{x}))Y^*_{nm}(\omega(\boldsymbol{y})).$$

Thus the matrix B is positive definite, and hence its maximum eigenvalue $\lambda_{\max}(B)$ can be bounded by

$$\lambda_{\max}(B) \le \mathrm{trace}(B) = \sum_{i=1}^{M}B_{i,i}.$$

By using the addition theorem for spherical harmonics, we can write $B_{i,i}$ as

$$\begin{aligned} B_{i,i} &= \sum_{n=0}^{\infty}\sum_{m=-n}^{n}[\widehat{\phi}(n)]^2(1+n^2)^sY_{nm}(\omega(\boldsymbol{x}_i))Y^*_{nm}(\omega(\boldsymbol{x}_i)) \\ &= \sum_{n=0}^{\infty}[\widehat{\phi}(n)]^2(1+n^2)^s\frac{(2n+1)}{4\pi}P_n(1), \end{aligned}$$

which is a convergent series because $\widehat{\phi}(n) \simeq (1+n^2)^{-\tau}$ and $\tau > s+1$. Thus

$$\lambda_{\max}(B) \le CM,$$

where the constant C is independent from N and the set X. This together with (3.16) and (3.17) yields

$$\max_{v\in V^\tau}\frac{|D_N(u,v)-D(u,v)|}{[D_N(v,v)]^{1/2}} \le CN^{-2s+1}\sqrt{M}\|u\|_{H^s(\Gamma_0)}.$$

This completes the proof of the theorem. □

ν	$\phi_\nu(r)$	τ
2	e^{-r}	1.5
3	$e^{-r}(1+r)$	2.5

Table 1: Matérn's RBFs

4 Implementation of the approximation method

The computation of the stiffness matrix A requires the computation of the functions H_n^m; see (3.11). These functions are defined from associated Legendre functions of the second kind Q_n^m. It is known (cf. [8]) that

$$(x^2-1)\frac{d}{dx}Q_n^m(x) = (n-m+1)Q_{n+1}^m(x) - (n+1)xQ_n^m(x).$$

Therefore the term $H_n^m(\cosh\mu_0)$ in the entry $A_{i,j}$ of the stiffness matrix (see (3.11) and (2.7)) can be computed by using the relation

$$H_n^m(x) = -(n-m+1)Q_{n+1}^m(x)/Q_n^m(x) + (n+1)x, \quad m = 0,1,\ldots,n;\ n = 0,1,2,\ldots$$

For negative values of m we use the relation $H_n^m(x) = H_n^{-m}(x)$.

The right hand side terms g_j are computed by using the Fourier coefficients of g and Φ_j, and Parseval's identity.

In our experiments, with no specific reasons, we used five different kernels $\Psi(\boldsymbol{x},\boldsymbol{x}') = \Phi(\omega(\boldsymbol{x}),\omega(\boldsymbol{x}'))$, where the functions Φ are restrictions to the sphere of two different classes of positive definite RBFs defined by Matérn and Wendland functions. Of course, other shape functions which define positive definite kernels can be used.

The Matérn functions (or Sobolev splines) were introduced for statistical applications in [7]. They are defined by

$$\phi_\nu(r) = \frac{2^{1-\nu}}{\Gamma(\nu)} r^{\nu-3/2} K_{\nu-3/2}(r), \quad \nu > 3/2,$$

where K_ν is the K-Bessel function of order ν. In $\mathbb{R}^3$, the Fourier transform of $\Psi(\boldsymbol{x}) = \phi_\nu(\|\boldsymbol{x}\|)$ decays like

$$\widehat{\Psi}(\xi) \sim (1+\|\xi\|_2^2)^{-\nu}.$$

The Matérn kernels used in our experiments are listed in Table 1. When restricting to the sphere, the native space associated with the kernel $\Phi(\boldsymbol{y},\boldsymbol{z}) := \phi_\nu(\sqrt{2-2\boldsymbol{y}\cdot\boldsymbol{z}})$ is the Sobolev space $H^{\nu-1/2}(\mathbb{S}^2)$ ([10]).

The Wendland functions [18] are positive definite functions with compact support. For any non-negative integer m, let

$$\widetilde{\rho}_m(r) = \begin{cases} (1-r)^{m+2}, & 0 < r \le 1, \\ 0, & r > 1, \end{cases}$$

and

$$\rho_m(r) = I^m \widetilde{\rho}_m(r), \quad r \geq 0,$$

where I is a smoothing operator on the space $C_K[0,\infty)$ of continuous functions in $[0,\infty)$ with compact supports defined by

$$I : C_K[0,\infty) \to C_K[0,\infty), \quad Iv(r) = \int_r^\infty sv(s)ds, \quad r \geq 0.$$

For arbitrary $\boldsymbol{y}, \boldsymbol{z} \in \mathbb{S}^2$,

$$\Phi(\boldsymbol{y}, \boldsymbol{z}) = \rho_m(\sqrt{2 - 2\boldsymbol{y} \cdot \boldsymbol{z}}),$$

with ρ_m being defined as above. It is shown by Narcowich and Ward [11] that in this case (3.5) holds for $\tau = m + 3/2$. The Wendland functions used in our experiments are listed in Table 2.

m	$\rho_m(r)$	τ
0	$(1-r)_+^2$	1.5
1	$(1-r)_+^4(4r+1)$	2.5
2	$(1-r)_+^6(35r^2+18r+3)$	3.5

Table 2: Wendland's RBFs

5 Numerical experiments

In our experiments we chose the prolate spheroid Γ_0 such that $f_0 = 4$ and $\mu_0 = 1$.
Example 1: Let the Neumann condition be

$$g(\mu,\theta,\varphi) = -\frac{1}{4f_0^4\sqrt{\cosh^2\mu - \cos^2\theta}} \frac{\sqrt{2}\sin 2\theta \cos\varphi(7 - 3\cosh 4\mu + 4\cosh 2\mu \cos 2\theta)}{(\cosh 2\mu + \cos 2\theta)^{7/2}}$$

so that the exact solution to (2.2) is

$$U(\mu,\theta,\varphi) = \frac{\sqrt{2}\sinh 2\mu \sin 2\theta \cos\varphi}{2f_0^3(\cosh 2\mu + \cos 2\theta)^{5/2}}. \tag{5.1}$$

This example is taken from [6] where the authors solve (2.6) using piecewise bilinear functions on grids of $\Lambda = \{(\theta,\varphi) : 0 \leq \theta \leq \pi,\ 0 \leq \varphi \leq 2\pi\}$.

Example 2: Let the Neumann condition be

$$g(\mu,\theta,\varphi) = -\frac{1}{f_0^3\sqrt{\cosh^2\mu - \cos^2\theta}} \frac{\cosh\mu \sin\theta \cos\varphi(-2\sinh^2\mu + \cos^2\theta)}{(\sinh^2\mu + \cos^2\theta)^{5/2}}$$

so that the exact solution to (2.2) is

$$U(\mu, \theta, \varphi) = \frac{\sinh\mu \sin\theta \cos\varphi}{f_0^2(\sinh^2\mu + \cos^2\theta)^{3/2}}. \tag{5.2}$$

We solved (3.9) in the space V^τ defined in (3.8) with three different types of sets of points X.

Points of type 1. As in [6], we divide the intervals $[0, \pi]$ and $[0, 2\pi]$ into N_1 and N_2 subintervals, respectively, by

$$\theta_s = s\pi/N_1, \quad s = 0, 1, 2, \dots, N_1,$$

and

$$\varphi_t = 2t\pi/N_2, \quad t = 0, 1, 2, \dots, N_2.$$

Then we use $M := N_2(N_1 - 1)$ points on Γ_0,

$$\boldsymbol{x}_{(N_2-1)s+t} = (f_0 \sinh\mu_0 \sin\theta_s \cos\varphi_t, f_0 \sinh\mu_0 \sin\theta_s \sin\varphi_t, f_0 \cosh\mu_0 \cos\theta_s),$$

where $1 \le s \le N_1 - 1$ and $1 \le t \le N_2$ to construct the basis functions.

Points of type 2. Next, we generate sets of points X on Γ_0 as images under the mapping ω, see (3.6), of sets of points $Y = \{\boldsymbol{y}_1, \dots, \boldsymbol{y}_M\}$ on $\mathbb{S}^2$ which are defined by using Saff's algorithm [13]. This algorithm partitions $\mathbb{S}^2$ into M equal-area regions whose centre are $\boldsymbol{y}_1, \dots, \boldsymbol{y}_M$; see Figure 3.

Points of type 3. Finally, we use sets of scattered points on the prolate spheroid which are obtained by mapping to the prolate spheroid the geocentric coordinates of data points taken from MAGSAT satellite data; see Figure 4. These sets are extracted from a full data set of about 26 million points in such a way that the separation radius of each set

$$q_Y = \frac{1}{2}\min_{\boldsymbol{y}\neq\boldsymbol{y}'} \cos^{-1}(\boldsymbol{y}\cdot\boldsymbol{y}')$$

is not too small; see Table 6. The minimum eigenvalue of the matrix A will depend on q_Y, the smaller the value of q_Y, the smaller the minimum eigenvalue of A.

The code was written in FORTRAN 90 and run on computers equipped with two Intel Xeon X5472 3.0GHz CPU. We used the `-parallel` compiling option and let the program run on 2 CPUs requesting 4GB RAM. We solved the matrix equation (3.10) by the conjugate gradient method with relative tolerance 10^{-8}, i.e. the stopping criterion is

$$\frac{\|A\boldsymbol{c}^{(m)} - \boldsymbol{g}\|_{l^2}}{\|\boldsymbol{g}\|_{l^2}} \le 10^{-8}.$$

Here $\boldsymbol{c}^{(m)}$ is the mth iterate.

Let $e := u - u_X$, where $u(\theta, \varphi) = U(\mu_0, \theta, \varphi)$ is the solution to (2.6) and u_X is the solution to (3.9). Here U is given by (5.1) and (5.2). We computed $\|e\|_{L^2(\Gamma_0)}$ and

$\|e\|_{H^{1/2}(\Gamma_0)}$ approximately by

$$\|e\|_{L^2(\Gamma_0)} \approx \left(\sum_{n=0}^{120} \sum_{m=-n}^{n} |\widehat{(u_X)}_{nm} - \widehat{u}_{nm}|^2 \right)^{1/2}$$

and

$$\|e\|_{H^{1/2}(\Gamma_0)} \approx \left(\sum_{n=0}^{120} (1+n^2)^{1/2} \sum_{m=-n}^{n} |\widehat{(u_X)}_{nm} - \widehat{u}_{nm}|^2 \right)^{1/2}$$

in which

$$\widehat{(u_X)}_{nm} = \sum_{i=1}^{M} \widehat{\phi}(n) c_i Y_{nm}(\omega(\boldsymbol{x}_i))$$

and $\widehat{u}_{nm}$ is computed by using a quadrature [3] for formula (2.3).

We also computed ℓ_2 and ℓ_∞ errors for point sets of type 1. Let $\mathcal{G}$ be points of the grid of size $(N_1, N_2) = (160, 320)$, then

$$\|e\|_{\ell^\infty(\Gamma_0)} = \max_{y \in \mathcal{G}} |u_X(y) - u(y)|$$

and

$$\|e\|_{\ell^2(\Gamma_0)} = \left(\frac{1}{|\mathcal{G}|} \sum_{y \in \mathcal{G}} |u_X(y) - u(y)|^2 \right)^{1/2}$$

where $|\mathcal{G}| = 50880$ is the cardinality of $\mathcal{G}$.

The numbers in Table 3 show fast convergence of our RBF Galerkin method applied to the Poincaré-Steklov operator with different values of N on different grids of size (N_1, N_2).

Table 4 shows the experimental orders of convergence (EOC) for the errors in the $H^{1/2}(\Gamma_0)$-norm (energy norm) when Saff points (points of type 2) and Wendland's kernels are used. Table 5 shows corresponding results when Matérn kernels are used. The value $N = 100$ is used throughout all experiments.

Table 6 gives the errors in the $L^2(\Gamma_0)$ and $H^{1/2}(\Gamma_0)$ norms for scattered points (points of type 3). In this case, the matrix is ill conditioned and hence a preconditioner is required. By noting (2.7) and (3.15), we can see that the symbol of the operator $\mathcal{K}$ defined in (2.4) behaves like $(n^2+1)^{1/2}$. Hence $\mathcal{K}$ is a pseudodifferential operator of order 1. This allows us to extend our analysis [17] for the overlapping Schwarz preconditioner on the sphere to the prolate spheroid. The preconditioner is defined by the additive Schwarz operator, using a subspace decomposition of V^τ as

$$V^\tau = V_0 + \cdots + V_J.$$

These subspaces V_j, $j = 0, \ldots, J$, are defined from a decomposition of the set Y into overlapping subsets Y_j, $j = 0, \ldots, J$. These subsets are generated by the following algorithm:

Select $\alpha \in (0, \pi/3)$, $\beta \in (0, \pi]$;
$\boldsymbol{p}_1 = \boldsymbol{y}_1 \in Y$;
$Y_0 := \{\boldsymbol{p}_1\}$;
$Y_1 := \{\boldsymbol{y} \in Y : \cos^{-1}(\boldsymbol{y} \cdot \boldsymbol{p}_1) \leq \alpha\}$;
$J = 1$, $k = 1$;
while $Y_1 \cup \cdots \cup Y_k \neq Y$ **do**
  $k = k + 1$;
  $\boldsymbol{p}_k$ is chosen from $Y \setminus Y_0$ such that $\cos^{-1}(\boldsymbol{p}_{k-1} \cdot \boldsymbol{p}_k) \geq \beta$;
  $Y_0 := Y_0 \cup \{\boldsymbol{p}_k\}$;
  $Y_k := \{\boldsymbol{y} \in Y : \cos^{-1}(\boldsymbol{y} \cdot \boldsymbol{p}_k) \leq \alpha\}$
end
$J = k$.

Each set Y_k is a collection of points inside a spherical cap of radius α centered at $\boldsymbol{p}_k$. These sets define subdomains on the prolate spheroid. The centers $\boldsymbol{p}_k$ are chosen so that the geodesic distance between two successive centers is no less than β, see Figure 5 for an illustration. This is to ensure that finally all points are considered, and thus the algorithm terminates. The set Y_0 serves as the coarse mesh in domain decomposition methods for finite element approximations. This set defines the space V_0 which provides global communication of data.

Table 7 shows the corresponding numbers of iteration of the preconditioned conjugate gradient using the same stopping criterion as before, i.e. with the relative tolerance $\leq 10^{-8}$. Errors of the same order as in the non-preconditioned case are obtained. The advantage of the preconditioner can be observed.

Acknowledgement

The paper was written when the second author was visiting the University of New South Wales. The support of the School of Mathematics and Statistics (UNSW) is acknowledged, as too is the support of the Australian Research Council under its Centres of Excellence Program. We are grateful to the anonymous referees for their constructive criticisms.

References

[1] M. Abramowitz and I. A. Stegun. *Handbook of Mathematical Functions with Formulas, Graphs, and Mathematical Tables.* Denver, New York, 1965.

[2] D. Chen, V. A. Menegatto, and X. Sun. A necessary and sufficient condition for strictly positive definite functions on spheres. *Proc. Amer. Math. Soc.*, 131:2733–2740, 2003.

N	m	(N_1, N_2)	$\|e\|_{L^2(\Gamma_0)}$	$\|e\|_{H^{1/2}(\Gamma_0)}$	$\|e\|_{\ell^2(\Gamma_0)}$	$\|e\|_{\ell^\infty(\Gamma_0)}$
20	0	(10, 20)	5.0800E-05	2.0340E-04	1.2060E-05	1.0370E-04
	0	(20, 40)	4.7470E-06	3.0590E-05	1.1420E-06	1.2750E-05
	0	(40, 80)	5.5490E-07	5.0730E-06	1.6220E-07	1.6620E-06
	0	(80,160)	5.0640E-10	2.4630E-09	3.5290E-08	2.0620E-07
	1	(10, 20)	1.8370E-05	6.4620E-05	4.4040E-06	1.6980E-05
	1	(20, 40)	2.3710E-07	1.4550E-06	5.6100E-08	3.3450E-07
	1	(40, 80)	7.0370E-09	5.9060E-08	2.0370E-09	1.1500E-08
	1	(80,160)	2.8680E-09	1.3010E-08	1.3320E-09	6.6860E-09
	2	(10, 20)	1.6380E-05	5.5680E-05	3.9940E-06	1.4670E-05
	2	(20, 40)	3.3650E-08	2.0250E-07	8.0110E-09	3.9520E-08
	2	(40, 80)	2.2970E-09	1.0430E-08	9.2740E-10	4.1430E-09
	2	(80,160)	2.2880E-09	1.0260E-08	9.2580E-10	4.1630E-09
40	0	(10, 20)	5.0980E-05	2.0330E-04	1.2120E-05	1.0190E-04
	0	(20, 40)	4.7490E-06	3.0580E-05	1.1420E-06	1.2780E-05
	0	(40, 80)	5.5490E-07	5.0730E-06	1.6220E-07	1.6620E-06
	0	(80,160)	6.4790E-10	2.9760E-09	3.5290E-08	2.0640E-07
	1	(10, 20)	1.8370E-05	6.4620E-05	4.4030E-06	1.6990E-05
	1	(20, 40)	2.3710E-07	1.4550E-06	5.6110E-08	3.3210E-07
	1	(40, 80)	7.0090E-09	5.8970E-08	1.9320E-09	1.1550E-08
	1	(80,160)	2.7980E-09	1.2580E-08	1.1630E-09	5.4830E-09
	2	(10, 20)	1.6380E-05	5.5680E-05	3.9940E-06	1.4670E-05
	2	(20, 40)	3.3650E-08	2.0240E-07	8.0100E-09	3.9240E-08
	2	(40, 80)	2.3080E-09	1.0470E-08	9.1070E-10	4.0000E-09
	2	(80,160)	2.2980E-09	1.0300E-08	9.0900E-10	3.9940E-09
80	0	(10, 20)	5.1010E-05	2.0330E-04	1.2120E-05	1.0170E-04
	0	(20, 40)	4.7510E-06	3.0580E-05	1.1420E-06	1.2690E-05
	0	(40, 80)	5.5500E-07	5.0730E-06	1.6220E-07	1.6620E-06
	0	(80,160)	6.4980E-10	2.9780E-09	3.5290E-08	2.0640E-07
	1	(10, 20)	1.8370E-05	6.4620E-05	4.4030E-06	1.6990E-05
	1	(20, 40)	2.3710E-07	1.4550E-06	5.6110E-08	3.3220E-07
	1	(40, 80)	6.4330E-09	5.7630E-08	1.5530E-09	1.0350E-08
	1	(80,160)	2.9350E-10	1.4560E-09	1.5540E-10	8.1760E-10
	2	(10, 20)	1.6380E-05	5.5680E-05	3.9940E-06	1.4670E-05
	2	(20, 40)	3.3650E-08	2.0240E-07	8.0100E-09	3.9250E-08
	2	(40, 80)	2.3080E-09	1.0470E-08	9.1050E-10	4.0000E-09
	2	(80,160)	2.2990E-09	1.0300E-08	9.0960E-10	4.0140E-09

Table 3: Errors on grid points with $\rho_m(r)$ as the RBF for Example 1

m	M	h_Y	$\|e_1\|_{H^{1/2}(\Gamma_0)}$	EOC	$\|e_2\|_{H^{1/2}(\Gamma_0)}$	EOC
0	100	0.2559	3.9114E-04		4.0634E-03	
	200	0.1798	1.1566E-04	3.45	1.5985E-03	2.64
	500	0.1127	3.4390E-05	2.60	4.9648E-04	2.50
	1000	0.0791	1.3579E-05	2.62	2.0009E-04	2.57
	2000	0.0563	5.4553E-06	2.68	8.3578E-05	2.57
	4000	0.0395	2.0215E-06	2.80	3.0819E-05	2.82
1	100	0.2559	2.4259E-04		1.5263E-03	
	200	0.1798	2.1280E-05	6.90	2.4034E-04	5.24
	500	0.1127	1.7924E-06	5.30	2.9786E-05	4.47
	1000	0.0791	3.2652E-07	4.81	5.9326E-06	4.56
	2000	0.0563	6.8446E-08	4.60	1.2448E-06	4.59
	4000	0.0395	1.3045E-08	4.68	2.3906E-07	4.66
2	100	0.2559	2.8762E-04		1.5340E-03	
	200	0.1798	1.1631E-05	9.09	9.7020E-05	7.82
	500	0.1127	2.8331E-07	7.95	4.5249E-06	6.56
	1000	0.0791	2.2296E-08	7.18	4.2003E-07	6.71
	2000	0.0563	2.3171E-09	6.66	4.5602E-08	6.53
	4000	0.0395	2.2211E-10	6.62	4.4375E-09	6.57

Table 4: Errors with Saff points and Wendland's RBF $\rho_m(r)$ for Example 1 ($\|e_1\|_{H^{1/2}}$) and Example 2 ($\|e_2\|_{H^{1/2}}$)

[3] J. R. Driscoll and D. M. Healy. Computing Fourier transforms and convolutions on the 2-sphere. *Adv. in Applied Math.*, 15:202–250, 1994.

[4] W. Freeden, T. Gervens, and M. Schreiner. *Constructive Approximation on the Sphere with Applications to Geomathematics.* Oxford University Press, Oxford, 1998.

[5] E. W. Grafarend, F. W. Krumm, and V. S. Schwarze, editors. *Geodesy: the Challenge of the 3rd Millennium*, Berlin, 2003. Springer.

[6] Hong-ying Huang and De-hao Yu. Natural boundary element method for three dimensional exterior harmonic problem with an inner prolate spheroid boundary. *J. Comput. Math.*, 24(2):193–208, 2006.

[7] Matérn. *Spatial Variation*, volume 36 of *Lecture Notes in Statistics.* Springer-Verlag, Berlin, 1986.

[8] Philip M. Morse and Herman Feshbach. *Methods of theoretical physics. 2 volumes.* McGraw-Hill Book Co., Inc., New York, 1953.

ν	M	h_Y	$\|e_1\|_{H^{1/2}(\Gamma_0)}$	EOC	$\|e_2\|_{H^{1/2}(\Gamma_0)}$	EOC
2	100	0.2559	3.9092E-04		1.8844E-03	
	200	0.1798	1.0909E-04	3.62	6.6891E-04	2.93
	500	0.1127	3.1312E-05	2.67	2.0206E-04	2.56
	1000	0.0791	1.2438E-05	2.61	8.1297E-05	2.57
	2000	0.0563	5.0249E-06	2.67	3.3334E-05	2.62
	4000	0.0395	1.8483E-06	2.82	1.2145E-05	2.85
3	100	0.2559	2.0555E-04		2.4005E-04	
	200	0.1798	1.5176E-05	7.38	3.8092E-05	5.22
	500	0.1127	8.4201E-07	6.19	2.8880E-06	5.52
	1000	0.0791	1.2202E-07	5.46	4.5335E-07	5.23
	2000	0.0563	2.3804E-08	4.81	9.1409E-08	4.71
	4000	0.0395	4.3470E-09	4.80	1.7398E-08	4.68

Table 5: Errors with Saff points and Matérn kernels $\phi_\nu(r)$ for Example 1 ($\|e_1\|_{H^{1/2}}$) and Example 2 ($\|e_2\|_{H^{1/2}}$)

m	M	q_Y	$\|e\|_{L^2(\Gamma_0)}$	$\|e\|_{H^{1/2}(\Gamma_0)}$	CPU	ITER
0	2133	$\pi/100$	1.08971E-6	7.79793E-6	19.2	1124
	7763	$\pi/200$	2.15172E-7	1.81600E-6	1592.3	7518
1	2133	$\pi/100$	3.76100E-8	2.54359E-7	102	7737
	7763	$\pi/200$	1.03461E-8	6.99365E-8	620.6	4059

Table 6: Errors with scattered points from MAGSAT data track using conjugate gradient method on Example 1 with $\rho_m(r)$ (CPU: computational times in seconds, ITER: numbers of iterations)

[9] C. Müller. *Spherical Harmonics*, volume 17 of *Lecture Notes in Mathematics*. Springer-Verlag, Berlin, 1966.

[10] F. J. Narcowich, X. Sun, and J. D. Ward. Approximation power of RBFs and their associated SBFs: a connection. *Adv. Comput. Math.*, 27:107–124, 2007.

[11] F. J. Narcowich and J. D. Ward. Scattered data interpolation on spheres: error estimates and locally supported basis functions. *SIAM J. Math. Anal.*, 33:1393–1410, 2002.

[12] J.-C. Nédélec. *Acoustic and Electromagnetic Equations*. Springer-Verlag, New York, 2000.

[13] E. B. Saff and A. B. J. Kuijlaars. Distributing many points on a sphere. *Math. Intelligencer*, 19:5–11, 1997.

m	M	$\cos\alpha$	$\cos\beta$	J	CPU	ITER	$\|e\|_{L^2(\Gamma_0)}$
0	2133	0.90	-0.01	42	4.4	68	0.11045E-5
	2133	0.80	-0.66	22	4.6	45	0.11045E-5
	2133	0.70	-0.78	17	5.6	36	0.11045E-5
	2133	0.60	-0.69	11	4.1	22	0.11045E-5
	7763	0.97	0.63	140	176.1	226	0.24240E-6
	7763	0.90	-0.46	48	133.6	85	0.24247E-6
	7763	0.80	-0.76	23	162.1	59	0.24239E-6
	7763	0.70	-0.84	17	238.2	51	0.24239E-6
1	2133	0.90	-0.01	42	10.9	251	0.36969E-7
	2133	0.80	-0.66	22	6.1	95	0.36969E-7
	2133	0.70	-0.78	17	7.9	75	0.36969E-7
	2133	0.60	-0.69	11	2.8	22	0.36969E-7
	7763	0.97	0.63	140	323.3	738	0.36654E-8
	7763	0.90	-0.46	48	104.5	147	0.42327E-8
	7763	0.80	-0.76	23	55.8	40	0.47790E-8
	7763	0.70	-0.84	17	154.8	60	0.35058E-8

Table 7: Computational times in seconds (CPU), numbers of iterations (ITER) and errors for overlapping additive Schwarz preconditioner on Example 1 with $\rho_m(r)$

[14] I. J. Schoenberg. Positive definite function on spheres. *Duke Math. J.*, 9:96–108, 1942.

[15] G. Strang and G.J. Fix. *An Analysis of the Finite Element Method.* Prentice-Hall, Englewood Cliffs, New Jersey, 1973.

[16] T. Tran, Q. T. Le Gia, I. H. Sloan, and E. P. Stephan. Boundary integral equations on the sphere with radial basis functions: Error analysis. *Appl. Numer. Math.*, 59:2857–2871, 2009.

[17] T. Tran, Q. T. Le Gia, I. H. Sloan, and E. P. Stephan. Preconditioners for pseudodifferential equations on the sphere with radial basis functions. *Numer. Math.*, 2010. In press. http://DOI 10.1007/s00211-009-0269-8.

[18] H. Wendland. *Scattered Data Approximation.* Cambridge University Press, Cambridge, 2005.

[19] Y. Xu and E. W. Cheney. Strictly positive definite functions on spheres. *Proc. Amer. Math. Soc.*, 116:977–981, 1992.

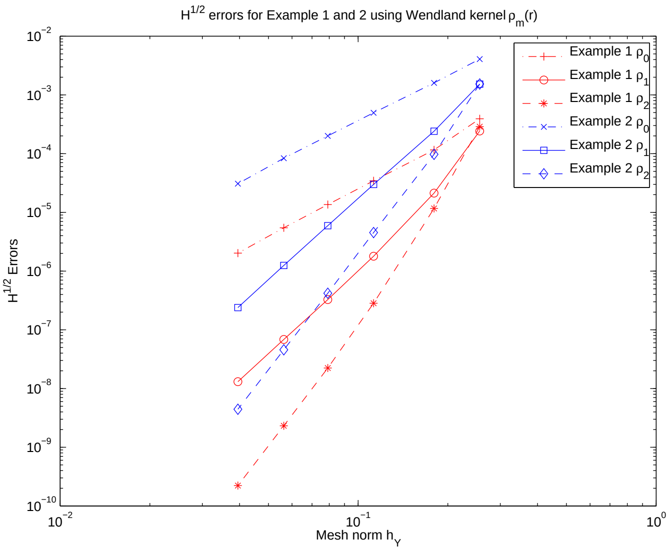

Figure 1: Log-log plot for $H^{1/2}(\Gamma_0)$ errors for Examples 1 and 2 using Wendland RBFs $\rho_m(r)$

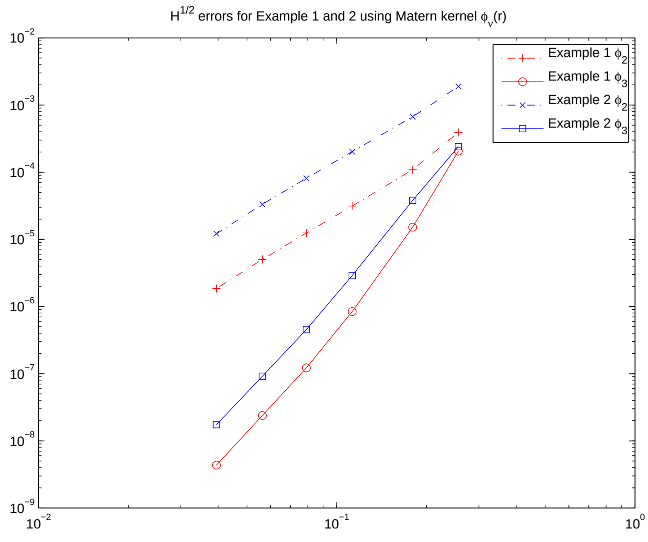

Figure 2: Log-log plot for $H^{1/2}(\Gamma_0)$ errors for Examples 1 and 2 using Matérn RBFs $\phi_\nu(r)$

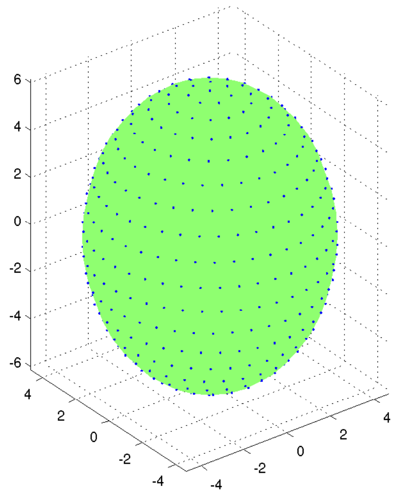

Figure 3: Image of Saff points on the prolate spheroid

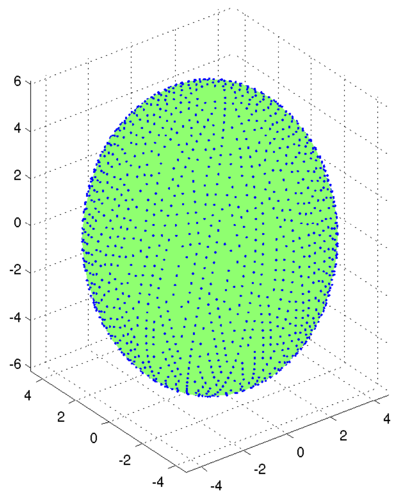

Figure 4: Image of satellite points on the prolate spheroid

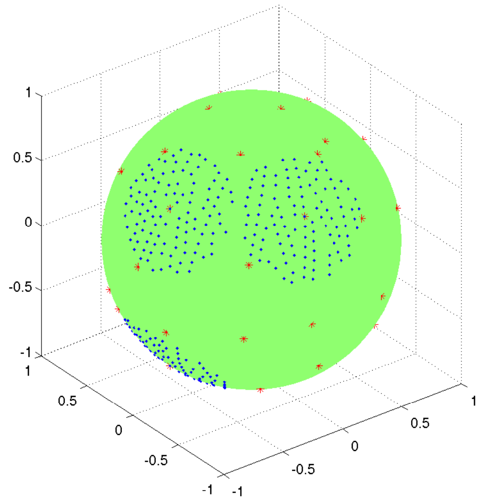

Figure 5: Subdomains on 2133 satellite points on the sphere, the centers are asterisked points

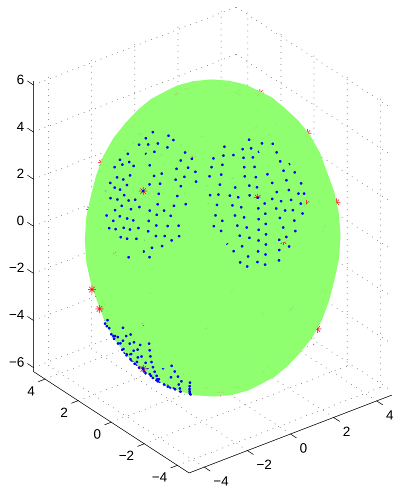

Figure 6: Subdomains get mapped to the prolate spheroid, the centers are asterisked points